ResearchGate

See discussions, stats, and author profiles for this publication at: https://www.researchgate.net/publication/231669206

Mechanism of Adsorption of Long−Chain Alkylamines on Silicates. A Spectroscopic Study. 1. Quartz§

ARTICLE *in* LANGMUIR · OCTOBER 2000

Impact Factor: 4.46 · DOI: 10.1021/la000254y

CITATIONS
53

READS
43

3 AUTHORS, INCLUDING:

Irina V Chernyshova
Columbia University
41 PUBLICATIONS **687** CITATIONS
SEE PROFILE

Vidyadhar Ari
National Metallurgical Laboratory
43 PUBLICATIONS **253** CITATIONS
SEE PROFILE

Available from: Vidyadhar Ari
Retrieved on: 25 January 2016

Mechanism of Adsorption of Long-Chain Alkylamines on Silicates. A Spectroscopic Study. 1. Quartz[§]

I. V. Chernyshova,* K. Hanumantha Rao,[†] and A. Vidyadhar

Division of Mineral Processing, Department of Chemical and Metallurgical Engineering, Luleå University of Technology, SE-971 87 Luleå, Sweden

A. V. Shchukarev

Department of Inorganic Chemistry, Umeå University, SE-901 87 Umeå, Sweden

Received February 23, 2000. In Final Form: June 8, 2000

The mechanism of adsorption of long-chain alkylamines at pH 6−7 onto quartz was studied using FTIR and XPS spectroscopy. The spectroscopic data were correlated with ζ potential and Hallimond flotation results. For the first time it was shown that (1) amine cation in the first monolayer is H-bonded with surface silanol group and this H-bond becomes stronger after the break in the adsorption characteristics (isotherm, ζ potential, floatability); (2) at the break the origin of the adsorbed amine species changes qualitatively, and along with alkylammonium ion attached to deprotonated silanol group, molecular amine appears at the surface and, as a result, monolayer thick patches of well-oriented and densely packed adsorbed amine species form rendering the surface highly hydrophobic; and (3) at higher amine concentration, bulk precipitation of molecular amine takes place. The counterion was found to influence both these steps. A model of successive two-dimensional and three-dimensional precipitation was suggested to explain amine adsorption on a silicate surface.

Introduction

The understanding of the mechanism of adsorption of long-chain alkylamines and elucidation of the properties of the adsorbed layers is important for a variety of industrial applications. In particular, primary long-chain alkylammonium salts are most commonly used for beneficiation of silicates,[1] principally because of their relatively high solubility. This problem was studied extensively by the electrokinetic, surface force, contact angle, and flotation recovery measurements during 1960−1980 (for reviews, see refs 2−4). At neutral and slightly acidic pH, alkylamines (weak electrolyte type surfactants) are almost totally ionized (for dodecylamine (DA) $pK_{a,aq} \approx 10.6$, $pK_{sol} \approx 8.41$[4]) while the silicate surface is negatively charged ($pH_{pzc} \approx 2-3$). Under these conditions and at low bulk amine concentration C_b (region I), the system is characterized by low adsorption of the surfactant, poor floatability, low contact angle, and practically constant or even decreasing to more negative values of ζ potential. It has been found[5,8] that the adsorbed amine ions are at greater distances apart (more than 1.34 nm^2/molecule) relative to the close-packed theoretical monolayer (ca. 0.25 nm^2/molecule) and adsorption area is proportional to hydrocarbon chain length. From a certain bulk concentration of amine (region II), the adsorption characteristics of the amine−mineral system steeply increase. At this critical concentration, surface coverage is 1−20% (19% for DA on quartz[8]) of the theoretical monolayer and ζ potential is still negative, i.e., the surface is essentially bare and a sufficient number of negative sites are still available.

A theory that is widely employed for interpretation of these regularities is due to Gaudin and Fuerstenau and is known as the hemimicelle model (HM).[6−9] It postulates that amine cations are attracted electrostatically to the oppositely charged surface but cannot readily displace water from the hydrophilic surface.[10] The invariance of ζ potential in region I is explained by replacement of positive ions (e.g., protons) in the *outer* Stern plane by amine cations. The adsorbed layer formed in such a manner is sporadic, and the orientation of the chains is chaotic, because of steric hindrance between the interacting hydrocarbon chains and electrostatic repulsion between

[§] Abbreviations: C_b bulk amine concentration; C_s, concentration at the mineral-solution interface; C_{pcr}, point of the charge reversal; C_s^{pcr}, surface concentration at point of the charge reversal; C_{sat}, 3D saturation concentration (bulk concentration at which solubility limit of molecular amine is achieved); C_{sol}, 3D solubility limit; C_{2D}, saturation concentration (surface concentration at which 2D solubility limit of molecular amine is achieved); C_{ref}, saturation concentration for the reference phase, parameter in the condensation theory (eq 8); C_{pr}, bulk concentration at which the 3330-cm^{-1} band of molecular amine appears in the DRIFT spectra; C_{mol}, bulk concentration at which the "H-bonded" band in the DRIFT spectra shifts from 3250 to 3000 cm^{-1}; $C_{sat,OH}$, bulk concentration up to which surface free silanol groups interact with adsorbed amine; T_K, the Krafft point; HM, hemimicelle model; CT, condensation theory; AT, admicelle theory; CHC, critical hemimicelle concentration; CMC, critical micelle concentration; DA, dodecylamine; HA, hexadecylamine; Ac, acetate.

* Author to whom correspondence should be addressed at the following: St. Petersburg State Technical University, Polytechnicheskaya 29, 195251 St. Petersburg, Russia; E-mail: Irina.Chernyschova@pobox.spbu.ru. Fax: +7(812)428-5712.

[†] E-mail: Hanumantha.Rao@km.luth.se.

(1) Leja, J. *Surface Chemistry of Froth Flotation*; Plenum Press: New York, 1982.

(2) Smith, R. W.; Scott, J. L. *Mineral Processing Extractive Metallurgy Rev.* **1990**, *7*, 81.

(3) Smith, R. W.; Akhtar, S. *Flotation*; A. M. Gaudin Memorial Volume; Fuerstenau, M. C., Ed.; American Institute of Mining Engineers: New York, 1976; Chapter 5, pp 87−116.

(4) Smith, R. W. *Reagents in Mineral Technology*; Somasundaran, P., Moudgil, B. M., Eds.; Marcel Dekker: New York, 1988; pp 219−256.

(5) Rutland, M.; Waltermo, A.; Claesson, P. *Langmuir* **1992**, *8*, 176.

(6) Gaudin, A. M.; Fuerstenau, D. W. *Trans. Soc. Min. Eng. AIME* **1955**, *202*, 958.

(7) Somasundaran, P.; Fuerstenau, D. W. *J. Phys. Chem.* **1966**, *70*, 90.

(8) Novich, B. E.; Ring, T. A. *Langmuir* **1985**, *1*, 701.

(9) Fuerstenau, D. W.; Jang, H. M. *Langmuir* **1991**, *7*, 3138.

(10) Hunter, R. J. *Zeta Potential in Colloid Science*; Academic Press: London, 1981, p 309.

10.1021/la000254y CCC: $19.00 © 2000 American Chemical Society
Published on Web 09/20/2000

the charged amino groups. In region II, the actual concentration of amine near the quartz surface (because of the gradient of the electrostatic potential) becomes higher than the critical micelle concentration (CMC) and a two-dimensional (2D) process similar to ordinary bulk (three-dimensional, 3D) micellization takes place. Namely, the decrease in free energy due to the removal of the hydrocarbon chains from water begins to override the energy increase due to the electrostatic repulsion between the positively charged headgroups. As a result, the surfactant aggregates at the surface and its adsorption is enhanced. This 2D aggregate is called hemimicelle (i.e., half of a micelle), and the critical concentration is referred to as the critical hemimicelle concentration (CHC). It is suggested[11,12] that in a hemimicelle hydrocarbon tails are oriented toward the solution while the headgroups are directed toward the surface.

Generality of the HM has been doubted by Smith,[2] who pointed out that at the temperature lower than the Krafft point T_K($T < T_K$) long-chain molecules are not flexible and mobile enough to form aggregates in solution and micelles cannot form. However, for DACl surface aggregation is observed at $T < T_K$ ($T_K = 26$ °C). For higher pH (7−8 < pH < 11) this discrepancy has been remedied by ascribing the adsorption enhancement to ordinary surface precipitation due to exceeding solubility limit of amines (2×10^{-5}M for DA at 25 °C[4]) within the quartz−solution interface[2] or to coadsorption of molecular amine.[13] In the latter case, the neutral molecules, building between the amine cations and screening the electrostatic repulsion between their headgroups, act as templates for the hemimicelle formation. However, this mechanism has been discarded[2] for lower pH since at pH < 7 the amine bulk concentration C_b at which the concentration of saturation, C_{sat}, is reached at the interface is higher than the threshold concentration of region II.[13] In addition, the HM cannot explain the following:

(1) why quartz is almost completely floated at a surface coverage of 2−6% monolayer at about neutral pH,[14] when the amine cations are "sparsely and chaotically" distributed, which implies low hydrophobicity of the surface; (2) why DACl is adsorbed up to about 20% of monolayer on fused silica at pH 3, where the adsorbent surface has relatively small negative charge;[15](3) why anionic surfactants are bound onto the clay minerals having an overall negative charge at all pHs; (4) why at pHs below pzc and concentrations of DA greater than 10^{-5} M, the quantity of the amine adsorbed on hematite is much greater than can be accounted for by attraction of amine ions at negatively charged surface sites and flotation of hematite with octadecylamine is observed below the pzc;[3,16] (5) why the adsorption isotherm of DA acetate (DAAc) on quartz at pH = 5 has no break at all;[17] and (6) why a higher flotation activity is shown by more hydroxylated quartz samples.[18]

To explain the adsorption isotherms of alkylammonium ions on biotite, phosphate oolite, and calcites, Cases et al.[19,20] have put forward the condensation theory (CT),

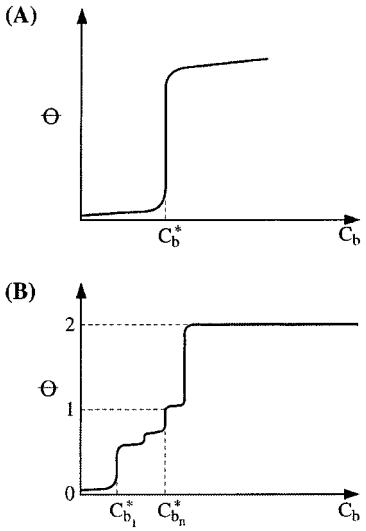

Figure 1. Scheme of Frumkin isotherm for (A) homogeneous and (B) heterogeneous surface at $\omega > 4kT$.

which is the basis of the admicelle theory (AT) by Scamehorn et al.[21] The main idea of the CT is that the break in the adsorption isotherm at CHC (Figure 1A) corresponds to 2D condensation of the surfactant at the interface. It is assumed that such a 2D phase is chemically identical to either the 3D hydrated crystal or micelles of the surfactant at $T < T_K$ or $T > T_K$, respectively. The CT is extended to any real (heterogeneous) surface, assuming that such a surface can be represented as a sum of homogeneous domains with different (specific) values of the 2D saturation concentration C_{2D}. Depending on the affinity to the surfactant, these domains are filled successively. As a result, the single jump in the isotherm (Figure 1, A) is broken into several jumps (Figure 1, B), which can be, however, experimentally undistinguishable. Nevertheless, these substeps have been observed in the isotherms of adsorption of alkylammonium chlorides on biotite,[22] phosphate oolite, and calcites.[19]

The CT predicts that with a further increase in the bulk concentration the second layer (bilayer) can form through the tail−tail interactions and ascribes to this process the most pronounced vertical step in the adsorption isotherm (Figure 1, B). After that the bulk saturation (3D condensation) takes place. Rao et al.[23,24] have found that the model of 2D condensation and 3D precipitation is able to describe the features on the adsorption isotherm of oleate on Ca minerals.

The advantage of the CT is in its generality. It differentiates the cases $T < T_K$ and $T > T_K$ and takes into account the adsorbate−adsorbent and adsorbate−adsorbate interactions and the possibility of the surface condensation. The CT includes the HM as the specific case of a homogeneous surface, $T > T_K$, and pure electrostatic adsorbate−adsorbent interactions.

The CT classifies affinity of the ionic surfactant to the surface as strong if the monolayer coverage is reached at a concentration much less than the CMC.[20] In this case, irrespective of the Krafft point, monolayer-thick patches

(11) Chandar, P.; Somasundaran, P.; Turro, N. J. *J. Colloid Interface Sci.* **1987**, *117*, 31.
(12) Somasundaran, P.; Healy, Th. W.; Fuerstenau, D. W. *J. Phys. Chem.* **1964**, *68*, 3562.
(13) Laskowski, J. S. *Challenges in Mineral Processing*; Sastry, K. V. S., Fuerstenau, M. C, Eds.; Society of Mineral Engineers: Littleton, 1989; p 15−34.
(14) Takeda, S.; Usui, S. *Colloids Surfaces* **1987**, *23*, 15.
(15) Nishimura, S.; Tateyama, H.; Tsunematsu, K. *J. Colloid Interface Sci.* **1993**, *159*, 198.
(16) Joy, A. S.; Watson, D. *Trans. IMM London* **1964**, *73*, 323.
(17) Takeda, S.; Usui, S. *Colloids Surf.* **1987**, *23*, 15.
(18) Chibowski, E.; Holysz, L. *Colloids Surf.* **1989**, *41*, 61.
(19) Cases, J. M.; Mutaftschiev, B. *Surf. Sci.* **1968**, *9*, 57.
(20) Cases, J. M.; Villieras, F. *Langmuir* **1992**, *8*, 1251.
(21) Scamehorn, J. F.; Schechter, R. S.; Wade, W. H. *J. Colloid Interface Sci.* **1982**, *85*, 463.
(22) Predali, J. J.; Cases, J. M. *Proc. 10th Int. Miner. Process. Congr. 1973* **1974**, 473−492.
(23) Hanumantha Rao, K.; Cases, J. M.; deDonato, P.; Forssberg, K. S. E. *J. Colloid Interface Sci.* **1991**, *145*, 314.
(24) Hanumantha Rao, K.; Cases, J. M.; Forssberg, K. S. E. *J. Colloid Interface Sci.* **1991**, *145*, 330.

with dense "crystalline-like" packing are predicted to form first, followed by the possibility of bilayer formation. Since the indicated relationship between the concentrations holds for adsorption of primary alkylamines at quartz, one should conclude that the amines are adsorbed at silicates strongly. At the same time, the formation of strong bonds between amine and a silicate in water under the conditions in question has not been confirmed spectroscopically yet. In contrast, indirect data[8,25] testify that DAAc is more likely adsorbed in form of disordered 3D micelle-like aggregates. In addition, like the HM, the CT neglects the possibility of the bulk precipitation of molecular amine and the effect of the surfactant counterion.

Recently, it has been found[26−29] that the origin of the counterion (more precisely, its affinity to the amine headgroup, and specific adsorptivity to the mineral surface) affect the adsorption of cationic surfactants. The X-ray photoelectron spectroscopy (XPS) study of adsorption of the halogen (Cl^-, Br^-, or I^-) salts of hexadecyltrimethylamine (CTA) on mica[26] has demonstrated clearly that formation of the first monolayer occurs in two distinct stages: (1) a fast nonequilibrium adsorption initial of the dipoles cation-negatively charged halogen counterion onto the negative-charged surface of mica to near monolayer saturation and (2) a second desorption of the mica surface counterions (K^+, Cs^+, or Ca^+) and halogen counterions from the surface. The oppositely charged counterions (halogen and metal) form ion pairs that proceed to slowly diffuse out of the headgroup region through the hydrophobic layer into the bulk solution, leaving behind the headgroups that are now bound to the surface more strongly via Coulombic (ionic) bonds than dipolar bonds. In the case of the larger and less hydrated Br, or I, ions the final adsorption of the amine was found to be less than that in the case of Cl^-. Since the binding energies of these anions to CTA^+ are in the order $I^- \gg Br^- > Cl^-$,[30] one can conclude that in the case under examination coadsorption of the counterion suppresses adsorption of the amine onto mica.

The effect of counterion is taken into account by the admicelle theory (AT).[31] The AT assumes that when a critical concentration is achieved the surfactant with the counterions aggregate in the vicinity of the surface in incomplete bilayers (flattened micelles), which are called admicelles. Formation of bilayer-shaped aggregates has been observed in solutions of CTA^+Br^- [32] and dihexadecyldimethylammonium salts.[26] However, the AFM study[33] of $C_{18}TA^+Br^-$ on mica at $T < T_K$ testifies to that this surfactant is adsorbed predominately as the monomer rather than as an aggregated solution species.

As follows from the numerous examples in the literature, the macroscopic characteristics of surfactant adsorption can be interpreted appropriately within the frameworks of different models (compare, e.g., interpretation of the same amine adsorption isotherms by Novich and Ring [8] and Cases et al.[20]). Only the data on the adsorbate structure as a function of bulk surfactant concentration can help one to select (or elaborate) the adequate theory of the surfactant adsorption.

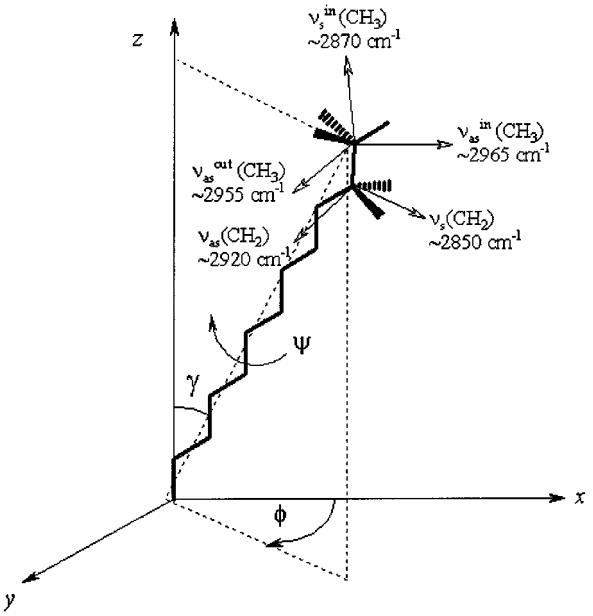

Figure 2. Definition of tilt γ, azimuth ϕ, and twist ψ angles for an all-trans hydrocarbon chain in the laboratory coordinate system and the stretching modes of methyl and methylene groups.

From very few spectroscopic studies on adsorption of amines on silicates, to the best of our knowledge, no one has employed IR spectroscopy. However, old traditional IR spectroscopy is well-known as a quick and nondestructive method which is very sensitive to the chemical and structural properties of the adsorbate. It has been widely used when studying the silica surface but in most cases, in the DRIFTS or transmission modes,[34] which, however, cannot provide information concerning orientation of adsorbed molecules. In contrast, the band intensities in the external reflection (also referred to as infrared reflection−absorption spectroscopy (IRAS)) measured at different angles of incidence and with different polarization states of radiation depend strongly on the orientation of the transition dipole moment (TDM) of the corresponding mode.[35]

As seen from Figure 2, in an all-trans conformation, the TDMs of the $\nu_s(CH_2)$ and $\nu_{as}(CH_2)$ modes of the hydrogen−carbon chains are orthogonal and both perpendicular to the carbon chain axis, the first TDM lying in the plane of the molecular CCC backbone and the other perpendicular to it. The terminal methyl group has three modes. The TDM of the symmetric mode ($\nu_{sym}^{ip}(CH_3) \approx 2870$ cm^{-1}) lies in the backbone plane and is inclined by 35.5° away from the molecular axis. One asymmetric stretch (near 2970 cm^{-1}), denoted by $\nu_{as}^{ip}(CH_3)$ is polarized 54.5° away from the molecular axis in the plane of the molecular backbone. Another asymmetric stretch (near 2954 cm^{-1}), denoted as $\nu_{as}^{op}(CH_3)$, is perpendicular to the plane of the molecular backbone (Figure 2).

(25) Chibowski, E.; Holysz, L. *Colloids Surfaces* **1989**, *41*, 61.
(26) Chen, Y. L.; Chen, S.; Frank, C.; Israelachvili, J. *J. Colloid and Interface Sci.* **1992**, *153*, 244.
(27) Scales, P. J.; Grieser, F.; Healy, T. W. *Langmuir* **1992**, *8*, 227.
(28) Koglin, E.; Tarazona, A.; Kreisig, S.; Schwuger, M. J. *Colloids Surfaces A* **1997**, *123−124*, 523.
(29) Bitting, D.; Harwell, J. H. *Langmuir* **1987**, *3*, 500.
(30) Lindman, B.; Wennerstrom, H. *Topics in Current Chemistry*; Springer-Verlag: New York, 1980; Vol. 87.
(31) Harwell, J. H.; Schechter, R.; Wade, W. H. *Solid−Liquid Interactions in Porous Media*; Colloque-Bilan, Nancy 6−10 fevrier 1984, Editions Technip: Paris, 1985, pp 371−409.
(32) Rennie, A. R.; Lee, E. M.; Simister, E. A.; Thomas, A. K. *Langmuir* **1990**, *6*, 1031.
(33) Hayes, W. A.; Schwartz, D. K. *Langmuir* **1998**, *14*, 5913.
(34) Vansant, E. F.; Van Der Voort, P.; Vrancken, K. C. *Characterisation and Chemical Modification of the Silica Surface*; Elsevier: Amsterdam, 1995.
(35) Horn, A. *Spectroscopy for Surface Science* Calrk, R. J. H., Hester, R. E., Eds.; John Wiley and Sons: New York, 1998; Vol. 26, pp 273−339.

Table 1. XPS Characterization of the Reagents and the Quartz Samples

sample	element atom % (BE, eV)			
	N	C	O	Si
solid DA	4.65 (399.5)	89.36 (285.0), 0.07 (286), 0.02 (287.7)	2.58 (531.2)	0
solid DAAc	1.46 (399.4), 3.78 (401.1)	76.19 (285), 5.66 (286.9), 3.94 (288.4)	7.99 (531.2), 0.99 (533)	0
fresh fracture of natural quartz	0	12.77 (285.0)	57.29 (532.8)	29.94 (103.6)
initial powder of natural quartz	0	13.12 (285.0)	57.35 (532.8)	29.55 (103.4)

It is well established[35,36] that the frequencies of the CH_2 stretching bands of hydrocarbon chains are extremely sensitive to the conformational ordering of the chains in a layer. When the chain is highly ordered (all-trans zigzag conformation), the narrow absorption bands appear at 2918 (CH_2^{as}) and 2848 cm^{-1} (CH_2^{s}) in the infrared spectrum of the layer, whereas if conformational disorder is included in the chains they shift upward to 2926 and 2856 cm^{-1}, depending upon the content of gauche conformers in the average orientation.[37] Although these frequency shifts are small, modern FTIR spectrometers permit their routine determination with a precision of better than ± 0.1 cm^{-1}. Along with the band frequency, the band bandwidth is very sensitive to molecule organization in a layer. It was found[38] that the bandwidth is proportional to the degree of the molecule mobility within the layer, increasing with temperature when the chain packing disorder increases.

One can further refine the details of chain packing by analyzing the shape and position of the methylene scissoring band $\delta(CH_2)$ (1460−1474 cm^{-1}).[39,40] It is established[40,41] that the single broad (fwhm $\approx$ 10−11 cm^{-1}) band at ca. 1466 cm^{-1} is characteristic of a relatively disordered hexagonal subcell packing where the hydrocarbon chain freely rotates around its long axis. The $\delta(CH_2)$ band is split into the doublet at 1473 and 1463 cm^{-1} due to intermolecular interaction between the two adjacent hydrocarbon chains in an orthorhombic perpendicular subcell, and the splitting is 5−8 cm^{-1} in the case of an orthorhombic inclined (∼30°) subcell. The splitting is expected[40,41] for molecular packing in the monoclinic (∼30° tilt) subcell. A sharp, narrow, and singlet band observed at 1471 cm^{-1} is indicative of a triclinic (most dense) the subcell packing where the hydrocarbon chains are packed in parallel arrangement.[42]

Another spectroscopic method that is employed in the present study is XPS. This method is inherently sensitive to the surface atomic composition, which makes it complimentary to the IR spectroscopy. The main advantage of XPS is that the binding energies (BE) of core level electrons depend on the atomic charges localized both on the ionized and the neighboring atoms, which can be used for characterizing of the charge redistribution at the surface.[43]

In silicate flotation practice, as a rule, acetate ammonium salts are used, while the previous studies of amine adsorption have been performed for both the acetate and halogen salts (see, e.g., the papers of Smith and Scott[2] and Novich and Ring[8]), without distinguishing the effect of the counterion. At the same time, it is well-known that acetate ion can be H-bonded[44] or even chemisorbed[45] onto a silicate surface.

Thus, the aim of the present work is elucidation of adsorption mechanism of primary alkylamines on one of the most common mineral, quartz (SiO_2), by using the FTIR and XPS spectroscopy.

Experimental Section

Reagents. Dodecylamine and hexadecylamine (HA) with purity of 99% were purchased from Fluka and Akzo Nobel, respectively. The acetate salts were synthesized by the standard procedure consisting in precipitation from the equimolar solution of amine and acetic acid in benzene. The amine acetate is insoluble in benzene at below the freezing temperature and it was purified thrice by recrystallization using fresh benzene each time. The XPS analysis (Table 1) reveals that nevertheless the acetate salts contain molecular form, as an impurity. Solutions of DAAc and HAAc were prepared by dissolving the necessary weight of the reagent in water. Naturally established pH was about 5.5, which then was adjusted by small quantities of NaOH. The solutions of DACl were prepared by continuous addition of the molecular amines and HCl into water so that the solutions were clear while pH was within the 6−7 range. Because HA is practically insoluble in water, it was first dissolved in ethanol. The stock aqueous solution of HAs contained 5% ethanol. Deionized water was used in all experiments.

Materials. As adsorbent, clear natural quartz crystals handpicked from the Mevior deposit (Greece) were used. A plate with dimensions of about 20 × 20 mm^2 was cut from a single crystal along the (002) crystallographic plane, which was checked by the XRD analysis. The working surface was prepared by successive polishing with the SiC papers down to 0.25 μm size and afterward thoroughly washing with deionized water. The XPS characterization of the fractured surface and the powder, which were used as adsorbents, is demonstrated Table 1. The quartz sample used in the present study was free from nitrogen impurity. To prepare powder the crystals were crushed, ground, and wet sieved to obtain the required size fractions (−5 μm and −150 + 38 μm). The finer size was obtained by microseiving in ultrasonic bath and employed for ζ potential measurements whereas the coarser size fraction was used for flotation tests. Specific surface areas (N_2−BET) was 0.09 and 1.30 m^2/g for the −150 + 38 μm and − 5 μm fractions, respectively. The ζ potential of the initial powder −5 μm size in deionized water at pH 6.5 was found to be −33 ± 2 mV.

Spectroscopic characterization. The FTIR spectra were obtained with a Perkin−Elmer 2000 spectrometer at 4 cm^{-1} resolution with a narrow band liquid N_2-cooled MCT detector. The IRRAS spectra were collected ex situ using an IRRAS accessory (Harrick, Inc.), by coadding 1000−1500 scans, both in s- and p-polarized radiation. To obtain the selected polarization, a wire-grid polarizer placed after the sample was used. The measurements were conducted immediately after the 5 min of conditioning of the quartz plate with the amine solution. The excess of the solution, if any, was removed carefully from the surface with a filter paper.

(36) Mendelsohn, R.; Brauner, J. W.; Gericke, A. *Annu. Rev. Phys. Chem.* **1995**, *46*, 305.
(37) Park, S. Y.; Franses, E. *Langmuir* **1995**, *11*, 2187.
(38) Katayama, N.; Enomoto, S.; Satao, T.; Ozaki, Y.; Kuramoto, N. *J. Chem. Phys.* **1993**, *97*, 6880.
(39) Snyder, R. G.; Liang, G. L.; Strauss, H. L.; Mendelsohn, R. *Biophys. J.* **1996**, *71*, 3186.
(40) Snyder, R. G. *J. Mol. Spectrosc.* **1961**, *7*, 116.
(41) Flach, C. R.; Gericke, A.; Mendelsohn, R. *J. Phys. Chem. B* **1997**, *101*, 58.
(42) Holland, R. F., Nielsen, J. R. *J. Mol. Spectrosc.* **1962**, *9*, 436.
(43) Ouyang, J.; Zheng, W.; Huang, N.; Tai, Z. *Thin Solid Films* **1999**, *340*, 257.
(44) Kubicki, J. D.; Schroeter, L. M.; Itih, M. J.; Nguyen, B. N.; Apitz, S. E. *Geochim. Cosmochim. Acta* **1999**, *63*, 2709.
(45) Eischens, R. P. *Science* **1964**, 146, 486.

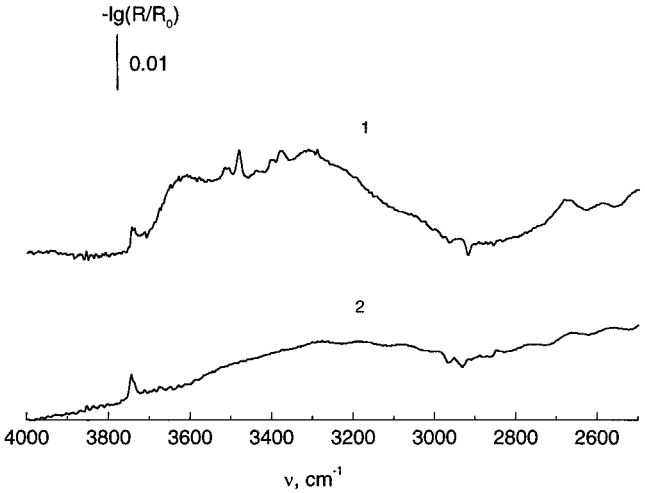

Figure 3. DRIFT spectra of (1) initial quartz and (2) quartz after 10 min treatment with in the HCl solution of pH 2. Both spectra were measured against KBr.

The DRIFT spectra were measured on the air-dried −5 μm powder after ζ potential measurements. The samples were not mixed with KBr since independent measurements revealed that dissolution lowers sensitivity of the DRIFT spectra with respect to adsorbed layers. This effect is explained by the fact that in the 4000−2000 cm^{-1} spectral range (where silicates do not have phonon bands) the role of the scattering transparent matrix is fulfilled by the silicate bulk. The untreated (initial) quartz powder was used as reference. The DRIFTS Perkin−Elmer accessory was utilized. Each spectrum is average of 500 scans.

The XPS spectra were recorded with AXIS Ultra (Kratos) electron spectrometer under Al mono irradiation with sample cooling. Vacuum in the sample analysis chamber during measurements was 10^{-8} Torr; 285.0 eV was adopted as the standard C(1s) binding energy.

The ζ potential measurements were made with Laser Zee Meter, Model 501 of Pen Kem Inc., equipped with a video system. All experiments were conducted at a pH of 6−7 and at normal laboratory atmosphere and temperature (20 ± 2 °C). Initially, a series of 100 mL of water or amine solutions with defined concentration preset to pH 6.5 were taken in Erlenmeyer flasks. Exactly 0.1 g of quartz powder was added into each of the flasks and the pH of the system was quickly adjusted to maintain the preset pH. The pH was measured with PHM 83 AUTOCAL pH meter (Radiometer Copenhagen) using a glass electrode calibrated with standard buffer solutions, also obtained from the same company. The mineral suspension was conditioned with magnetic stirrer for 1 h, during which time pH was monitored and adjusted if necessary to maintain the preset pH. The pH was adjusted by suitable concentration solutions of NaOH (for the solutions of amine acetates) or HCl (for the solutions of molecular amines). The mineral suspension was then filled into the ζ-meter rectangular cell. Upon applying suitable potential (generally 100 V), the ζ potential was recorded. After the measurement, the pH was again measured (if there was a large deviation, greater than ±0.5, to the preset pH 6.5, the measurement was discarded) and the suspension was filtered using Millipore filter paper (pore size 0.22 μm). The solids were allowed to air dry overnight at the room temperature, and the DRIFT spectra were recorded for all the air-dried samples after ζ potential measurements.

Flotation. The single mineral flotation tests were performed with a Hallimond flotation cell of 100 mL capacity. Initially, 1 g of the mineral was conditioned separately in 100 mL of predetermined concentration of amine solution and at given pH 6−7 for 5 min. The pulp was then transferred into the Hallimond cell for flotation for 1 min at the air flow rate of 8 mL/min.

Results

DRIFTS. Figure 3, curve 1 shows the DRIFT spectrum of the initial −5 μm quartz powder, which was used as reference while recording all of the DRIFTS spectra. The narrow band at 3745 cm^{-1} is unambiguously assigned to the stretching ν(O−H) vibrations of surface isolated silanol groups.[46,34] The complex structurized absorption band in the 3000−3700 cm^{-1} spectral region, due to adsorbed H-bonded hydroxyls and water, is typical for some types of natural fine quartz powders.[46] These observations are in agreement with the known fact that at pH 2−7 the quartz surface is covered mostly by hydroxyls, which bear the surface negative charge.[47]

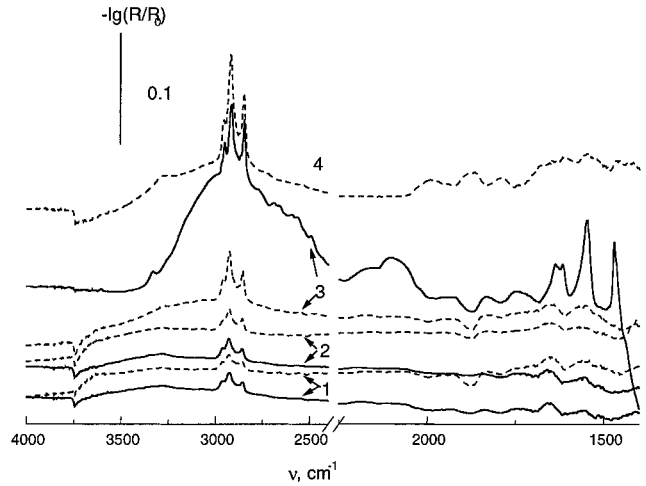

Figure 4. DRIFT spectra of quartz powder (5 μm size) after 1 h treatment with the DAAc (dashed lines) and DACl (solid lines) solution (pH 6−7) of concentration (1) 5×10^{-6} M; (2) 1×10^{-4} M; (3) 2×10^{-3} M; (4) 1×10^{-2} M. Spectrum (3) for DACl is divided by 5.

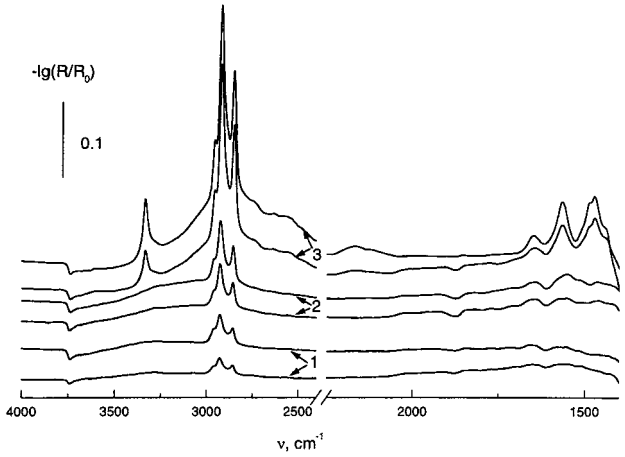

Figure 5. DRIFT spectra of quartz powder (−5 μm size) after 1 h treatment with the HAAc and HACl solution (pH 6−7) of concentration (1) 2×10^{-6} M; (2) 2×10^{-5} M; (3) 5×10^{-5} M. In the pairs of spectra, the upper spectra are due to HACl.

Figures 4 and 5 show selected spectra of the quartz treated with solutions of DA and HA of different initial concentrations (C_b). All display the typical bands in the 3000−2800 cm^{-1} range due to the ν(C−H) vibrations of alkyl chains. A broad structural band centered at ca. 3250−3000 cm^{-1} is attributed to the H-bonded $\nu(N^+-H)$, ν(O−H), and ν(N−H) (if any, vide infra) stretching vibrations. Inspection of this band reveals that it is located at ca. 3250 cm^{-1} at low and at ca. 3000 cm^{-1} at high C_b (Figure 6). It is well-known[48] that a red shift of any H-bonded stretching mode points to the H-bond strengthening.

(46) Coretsky, C. M.; Sverjensky, D. A.; Salisbury, J. W.; D'Aria, D. M. *Geochim. Cosmochim. Acta* **1997**, *61*, 2193.

(47) Stumm, W.; Morgan, J. J. *Aquatic Chemistry*, 3rd ed.; John Wiley and Sons: New York, 1996; p 579.

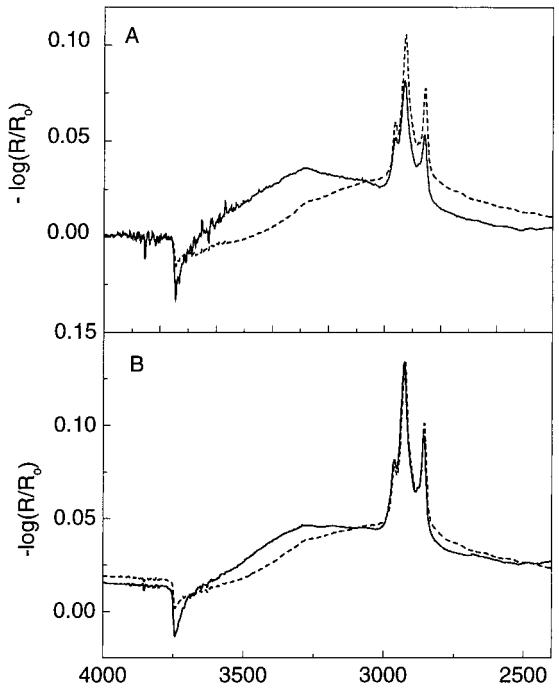

Figure 6. DRIFTS spectra of quartz conditioned with (A) DACl at 2×10^{-4} M (solid line, the spectrum is multiplied by 2.5) and 5×10^{-4} M (dashed line) and (B) HAAc at 1×10^{-5} M (solid line, the spectrum is multiplied by 2) and 2×10^{-5} M (dashed line).

Particular emphasis has to be placed on the fact that this phenomenon takes place abruptly at a certain value of C_b. These values marked as C_{mol} are listed in Table 2.

In all the spectra the negative 3745-cm^{-1} band of free surface silanols is observed. Its negative intensity means that silanols interact with the absorbed amine. It is natural to suggest that this interaction is H-bonding between a proton of the headgroup of amine cations and the SiOH oxygen. To verify that the specific interaction takes place for amine adsorption on a quartz surface, we measured the DRIFTS spectra of DACl adsorbed from the 2×10^{-4} M solution at pH 2 (pzc) (Figure 7, curve 1). Comparing this spectrum with the spectrum of DACl adsorbed from the 2×10^{-4} M solution at pH 6.5 (Figure 7, curve 2), one sees that even at pzc the amine is adsorbed and the quantity of adsorbed amine is proportional to the quantity of reacted free surface silanols. The presence of free silanols on the surface of quartz conditioned in the amine-free HCl solution of pH 2 is seen from Figure 3, curve 2.

In addition, adsorption of both the C_{16} amines at $C_b > 2 \times 10^{-5}$ M results in appearance of a series of new bands at 1650−1640, 1570, 1490 cm^{-1}, etc. At 5×10^{-5} M, the characteristic absorption band at 3330 cm^{-1} appears (Figures 4 and 5). In the case of DACl, these spectral features are observed only at 2×10^{-3} M, being undistinguishable in the case of DAAc at all (Figure 4). Comparison with the DRIFTS spectra of the molecular and protonated forms of amine (Figure 8 and Table 3) permits associating these "extra" bands with bulk phase of the molecular amine.

The results shown in Figures 9 and 10 allow one to follow how the surface coverage of the amines, the number of the interacted free silanol groups, and the molecular order correlate with each other and with ζ potential measured on the same sample. The surface coverage of the amine is proportional to the normalized intensity of the $\nu_{as}(CH_2)$ band, A_n, which is calculated as the band absorbance integrated within the 2945−2902 cm^{-1} range and divided by the number of the methylene units in the chain. These limits have been found to minimize contribution of the other ν(CH) vibrations.[49] The number of the reacted surface silanol groups is assumed to be proportional to the peak intensity, E, of the negative 3745-cm^{-1} band. The A_n curves are similar to the amine adsorption isotherms, e.g., to those reported by Schubert,[50] where DA exhibits two regions and HA displays three regions. By definition, the first break corresponds to CHC. As seen from Table 2, where the CHC values are collected, CHC is the same (2×10^{-5} M) for both HA, while for DA it is much lower for the acetate salt. The important fact is that CHC coincides with C_{mol} in all the cases, while the concentration of micro-phase precipitation of molecular amines, C_{pr}, is somewhat higher than CHC.

The E curves reach the plateau at a certain value of bulk amine concentration $C_{sat,OH}$ (Table 2). Obviously, at $C_b > C_{sat,OH}$ the quartz particles are totally screened from interaction with the solution by the adsorbed amine. The number of the "saturated" silanol groups (the plateau height) is higher in the case of the acetate salts. Since under the saturation conditions, the quantity of adsorbed amine is higher for the chloride salts (Figures 9 and 10, A), it can be deduced that this effect is due to coadsorption of acetate ion. Another conclusion drawn from the E curves is that the $C_{sat,OH} >$ CHC, in agreement with the other data.[2,3,8,17]

It is of importance that the progressive increase in the surface coverage of the amine is accompanied by a red shift of the $\nu(CH_2)$ bands (Figures 9 and 10, C). Attention is to be drawn to the fact that the beginning of this shift coincides with C_{mol} = CHC (Table 2). According to the correlation mentioned in the Introduction, this fact means that the order of the adsorbed layer increases at $C_b > C_{mol}$. The shifts reach its maximum when molecular amine precipitates at the surface. For HA, the frequency (2918.6 cm^{-1}) becomes close to that of the solid molecular amine. It follows that in the precipitates all of the chains are in the trans-zigzag conformation, being parallel to each other and densely packed. The case of DAAc stands out by the fact that at concentrations greater than 1×10^{-3} M, there is an additional weak 3010-cm^{-1} band in the ν(CH) region. This band can be assigned to the $\nu_{as}(CH_3)$ vibration of noncoordinated (ionic) acetate.[51] When acetate ion is coordinated (Figure 8, Table 3), this band is observed at substantially lower frequencies.[52]

XPS. The XPS measurements were conducted at several powdered samples for which the DRIFTS and ζ potential measurements are demonstrated in Figures 9 and 10, and at the fracture surface of the crystal quartz. The results are shown in Figures 11−13 and Table 4.

Adsorption of amines manifests itself in the XPS spectra as the following: (1) appearance of the N(1s) signal of the amino groups; (2) the 1.5−4-fold increase in the intensity of the C(1s) peak as compared to that of the initial surface (Table 1); (3) a decrease in the peak intensities of silicon and oxygen. Difference in adsorption of DACl and DAAc consists of that in the former case a weak Cl(2p) peak arises in the XPS spectrum of the sample conditioned at 2×10^{-4} M. Instead of this, the C(1s) peak of adsorbed DAAc is complex: the curve fitting distinguished the

(48) Pimentel, G. C., McClellan, A. L. *The Hydrogen Bond*; Freeman, San Francisco, CA, 1960.
(49) Kumar, V.; Krishnan, S.;. Steiner, C.; Maldarelli, C.; Couzis, A. *J. Phys. Chem. B.* **1998**, *102*, 3152.
(50) Schubert, H. *Freiberger Forschungshefte* A. **1972**, *514*, 3.
(51) Nakamoto, K. *Infrared and Raman Spectra of Inorganic and Coordination Compounds*, Part B, 5th ed.; John Wiley & Sons: New York, 1997; p 60.
(52) Karseboom, S. G.; Davis, J. E.; Mullins, C. B. *Surf. Sci.* **1997**, *383*, 173.

Table 2. Characteristics of Amine Adsorption on Quartz

amine	CHC, M	A_n[a]	C_{mol}, M[b]	C_{pr}, M[c]	C_{pcr}, M[d]	A_n	$C_{sat,OH}$, M[e]	E[f]
HACl	2×10^{-5}	0.049	2×10^{-5}	$>2 \times 10^{-5}$	2.3×10^{-5}	0.10	5×10^{-5}	0.014
HAAc	2×10^{-5}	0.075	2×10^{-5}	$>2 \times 10^{-5}$	5×10^{-5}	0.22	2×10^{-5}	0.015
DACl	$\sim 3 \times 10^{-4}$	0.057	$\sim 3 \times 10^{-4}$	2×10^{-3}	1.4×10^{-3}	0.21	4.4×10^{-4}	0.014
DAAc	7×10^{-4}	0.025	2×10^{-3}		2.2×10^{-3}	0.05	3×10^{-3}	0.015

[a] A_n= normalized integrated intensity of the $\nu_{as}(CH_2)$ band at the CHC or pcr concentration in cm^{-1}. [b] C_{mol} is the concentration, at which the absorption band of H-bonded ν(OH) and ν(NH) vibrations changes its position from ca. 3250 to ca. 3000 cm^{-1}. [c] C_{pr} is the concentration at which the 3330 cm^{-1}-band of bulk phase of molecular amine appears. [d] C_{pcr} is the concentration at which ζ potential reverses sign (point of charge reverse). [e] $C_{sat,OH}$ is the concentration at which the E curves in Figures 9 and 10 reach the plateau. [f] E = absolute value of peak absorbance of the negative band of surface isolated silanol groups. CHC is determined as the concentration at which the surface coverage abruply increases.

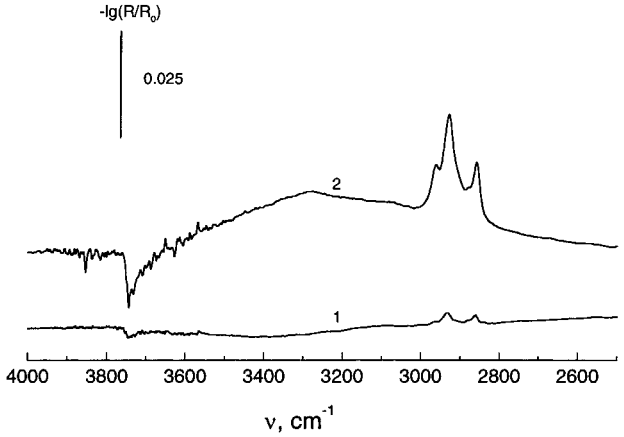

Figure 7. DRIFT spectra of quartz powder conditioned in the 2×10^{-4} M DACl solution (1) 10 min at pH 2 and (2) 1 h at pH 6.4.

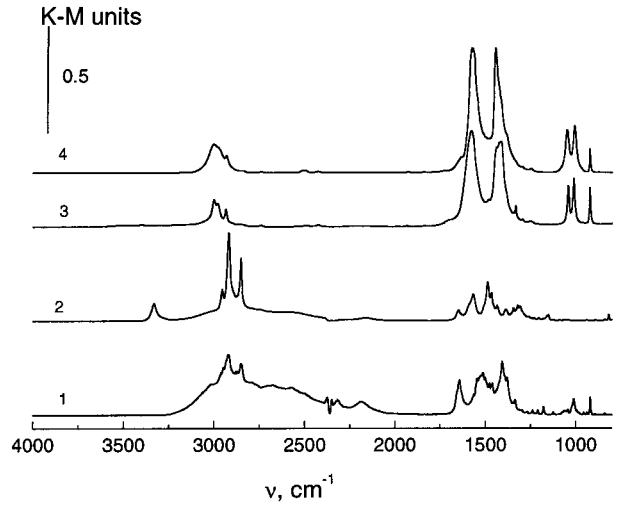

Figure 8. DRIFTS spectra of (1) DAAc; (2) DA; (3) $CH_3COONa \cdot 3H_2O$; and (4) CH_3COONa in KBr matrix. Asignment of the absorption bands is given in Table 4.

components at 286.8 and 288.6 eV (Figure 11, curves 2 and 3). The first component is assigned to carbon in the C−N and C−O bonds and the second one to carbon in the carboxylate group.[53] These data testify that acetate and chlorine ions are coadsorbed physically with the corresponding amines, the coadsorption of acetate anion being higher. From the atomic ratios calculated from the whole N(1s) peak and the 288.6-eV component of the C(1s) peak, it follows that at $C_b = 2 \times 10^{-4}$ M one amine cation is coadsorbed approximately by one acetate anion.

An important aspect to be clarified is the character of interaction between the amine headgroup and surface silanols at amine bulk concentration equal to and lower than CHC. As seen from Figure 12, curves 1 and 2 and Table 4, the amines adsorbed at powdered quartz at $C_b \approx$ CHC are characterized by the N(1s) peak consisting of two components with BE of 399.5 ± 0.1 and 401.5 ± 0.1 eV. Comparing these values with BEs of amino and ammonium groups in crystalline DA and DAAc, respectively (Table 1), one can arrive at the conclusion that the adsorbed layer is comprised of molecular alkylamine and alkylammonium ion. However, the BE of the N(1s) core level electron of ammonium at the quartz surface (401.5 eV) is marginally higher than that in the crystalline alkylammonium acetate (401.1 eV). A probable explanation for this fact is that at the surface ammonium group is coordinated to the species with a higher proton affinity than that in the acetate salt. It is reasonable to suggest that these species are negatively charged (deprotonated) oxygen atoms.

Kowalczyk et al.[54] have reported the N(1s) spectra of aminopropyltriethoxysilane adsorbed from toluene on the hydroxylated surface of fused quartz by amino group. These spectra exhibit two peaks with BE at 400.1 and 402.1 eV. The first component has been attributed to the amino group H-bonded with surface silanol, while the second component has been attributed to the ammonium group formed due to charge transfer in a strong H-bond between nitrogen of an amino group and a silanol group:

$$RNH_2 \cdots HOSi\equiv \Leftrightarrow RNH_3^+ \cdots {}^-OSi\equiv \qquad (1)$$

The meaning of this result is that once molecular amine acting as a base forms H-bond with surface silanol group acting as an acid, equilibrium (1) is established at the surface. On the basis of this conclusion and the BE values of the N(1s) core level electrons of alkylamines adsorbed on quartz, which were obtained in the present work, we suggest that at $C_b \approx$ CHC molecular amine appears at the surface, establishing equilibrium (1) between the molecular and protonated form.

The striking feature is that at $C_b <$ CHC (DAAc at $C_b = 2 \times 10^{-4}$ M and DACl at $C_b = 4 \times 10^{-5}$ M), the N(1s) spectrum constitutes the single peak with BE 400.1 eV (Figure 12, curve 3). Since this BE is intermediate between those in the molecular and protonated form in equilibrium (1), we conclude that most probably in this case the ammonium group is H-bonded as

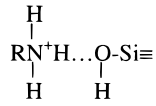

(2)

In general the NH···O bonds are weaker than the N···HO bonds[48] and proton-donating property of surface silanol groups is higher than its proton-accepting property in the H-bonding with a water molecule and acetic acid/acetate ion pair.[55] Thus, the transition from species (2) to

(53) Moulder, J. F. *Handbook of X-ray Photoelectron Spectroscopy*; Perkin-Elmer Co.: Physical Electronics Division, USA, 1995.

Table 3. Assignment of the Major Absorption Bands in the DRIFT Spectra of the Reagents in Solid Form (Figure 8)

$C_{12}H_{23}NH_2$[77,78,79]		$C_{12}H_{23}NH_3^+Ac^-$ [46,47]		$CH_3COONa\cdot3H_2O$[46,47]	
ν, cm^{-1}	mode	ν, cm^{-1}	mode	ν, cm^{-1}	mode
3333	$\nu_{as}(NH_2) + \nu_s(NH_2)$ in NH···N H-bonds	~3000 (br)	$\nu_{as}(NH_3^+)$		
		~2600 (br)	$\nu_s(NH_3^+)$		
2956	$\nu_{as}(CH_3)$	2963	$\nu_{as}(CH_3)$ (Ac^-)	3002	
2920	$\nu_{as}(CH_2)$	2950	$\nu_{as}(CH_3)$	2981	$\nu(CH_3)$
2873	$\nu_s$in(CH_3)	2933	$\nu_{as}(CH_3)$ (Ac^-)	2936	
2852.5	$\nu_s(CH_2)$	2921.6	$\nu_{as}(CH_3)$		
		2900	$\nu_s(CH_2)$ FR[a]		
		2890	$\nu_s(CH_2)$ FR[a]		
		2870.7	$\nu_s^{ip}(CH_3)$		
		2851.6	$\nu_s(CH_2)$		
1650	$\delta_{as}(NH_2) + \delta(H_2O)$	1645	$\nu_{as}(COO^-)(Ac^-) + \delta(H_2O)$		
1570	$\delta_s(NH_2)$	1544	$\delta_{as}(NH_3^+) + \delta(H_2O)$		
1490	?	1520	$\delta_s(NH_3^+)$	1580	$\nu_{as}(COO^-)$
1470	$\delta(CH_2)$	1460−1480	$\delta(CH_2)$	1445	$\nu_s(COO^-)$
1388	$\omega(CH_2)$	1407	$\nu_s(COO^-)(Ac^-)$		
1153	$\rho(NH_2)$	1337			
				1051	$\rho(CH_3)$
		1010	$\rho(CH_3)(Ac^-)$	1007	
		920	ν(C−C)(Ac^-)	923	ν(C−C)

[a] FR = Fermi resonance components of the band coupling with overtone of $\delta(CH_3)$.

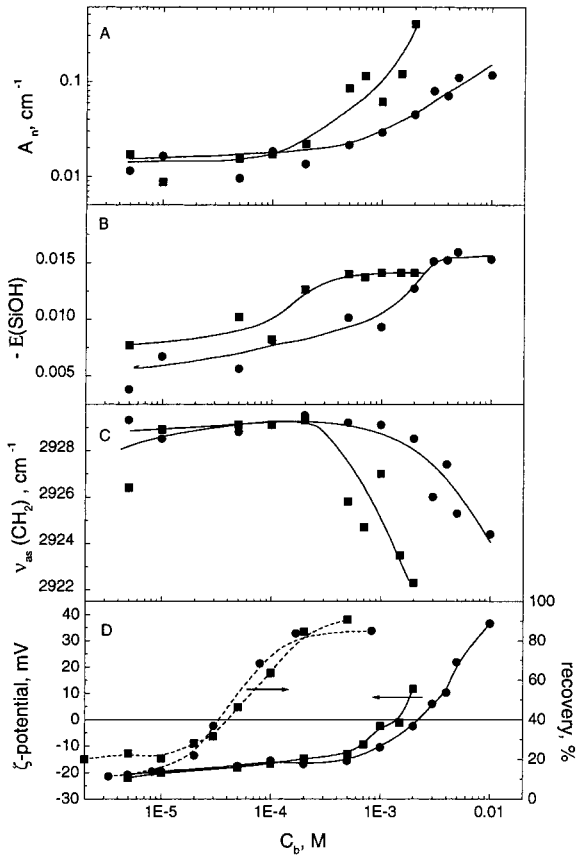

Figure 9. Adsorption characteristics of DAAc (●) and DACl (■) at powder quartz at pH 6−7 and $t = 20$ °C. (A) Normalized integrated intensity $A_n = A/11$ cm^{-1}, of the $\nu_{as}(CH_2)$ band; (B) peak intensity of the absorption band at 3745 cm^{-1} of silanol groups; (C) frequency of the $\nu_{as}(CH_2)$ band; (D) ζ potential (solid lines) and flotation recovery (dashed lines) as a function of bulk amine concentration.

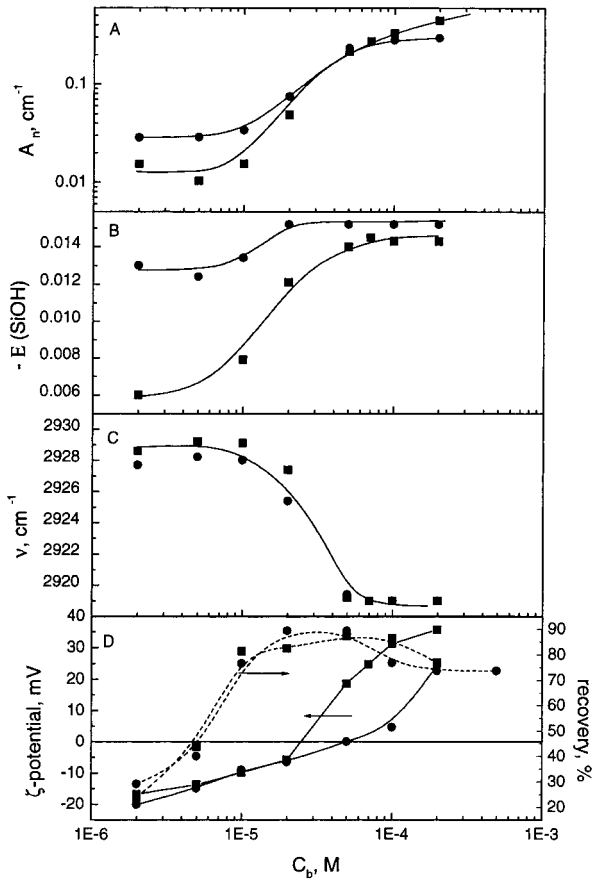

Figure 10. Adsorption characteristics of HAAc (●) and HACl (■) at powder quartz at pH 6−7 and $t = 20$ °C. (A) Normalized integrated intensity, $A_n = A/15$ cm^{-1}, of the $\nu_{as}(CH_2)$ band; (B) peak intensity of the absorption band at 3745 cm^{-1} of silanol groups; (C) frequency of the $\nu_{as}(CH_2)$ band; (D) ζ potential (solid lines) and flotation recovery (dashed lines) as a function of bulk amine concentration.

species (1) should be accompanied by red shift of the corresponding "H-bonded" band in the IR spectra. This indeed happens at CHC (Figure 6), supporting the above assignment of the N(1s) spectra.

We regard the following experimental facts as an indirect confirmation of the rather strong bonding between primary amines and quartz at concentrations well below and above CHC. To obtain the XPS spectrum of crystalline

(54) Kowalczyk, D.; Slomkowski, S.; Chehimi, M. M.; Delamar, M. *Int. J. Adhesion Adhesives* **1996**, *16*, 227.
(55) Kubicki, J. D.; Blake, G. A.; Apiz, S. E. *Geochim. Cosmochim. Acta* **1997**, *61*, 1031.

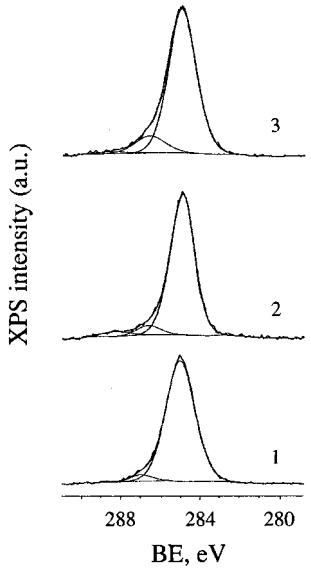

Figure 11. XPS C(1s) spectra of quartz powder conditioned with (1) 2×10^{-4} M DACl; (2) 2×10^{-4} M DAAc; and (3) 2×10^{-5} M HACl.

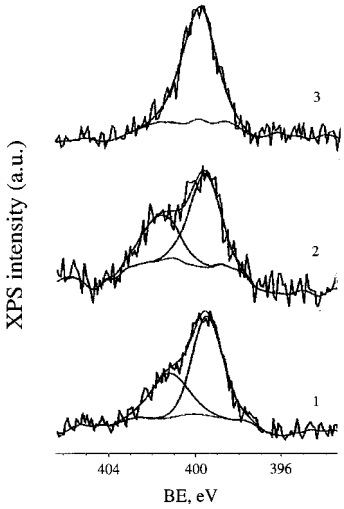

Figure 12. XPS N(1s) spectra of quartz powder conditioned with (1) 2×10^{-4} M DACl; (2) 2×10^{-4} M DAAc; and (3) 4×10^{-5} M DAAc.

DAAc, precooling was required. Otherwise, the sample flushed out totally during the first minutes of exposure to ultrahigh vacuum. At the same time, it was checked that the N(1s) peak intensity of adsorbed DACl decreased by 30% but not disappeared after heating the sample in the spectrometer chamber up to room temperature and keeping it warmed overnight (Table 4). Curiously, when both the ionic and molecular species were present at the surface and the sample was treated as described (Figure 13), the ionic species characterized by the 401.5-eV peak partly evaporated from the surface while the molecular species are bound so strongly to the surface that their concentration remained practically unchanged.

It is interesting to compare the N(1s) spectra for C_{12} amines adsorbed at the fracture surface and the powder from the solution of the same concentration $C_b = 2 \times 10^{-4}$ M, which is close to the CHC for the powder (Table 4). As opposite to the case of the powder, the N(1s) spectrum of the amines adsorbed at the fracture surface has the single peak at 400.1 eV. Therefore, CHC is lower for the adsorption of amines on powder as compared with that on the fracture sample. We explain this observation by

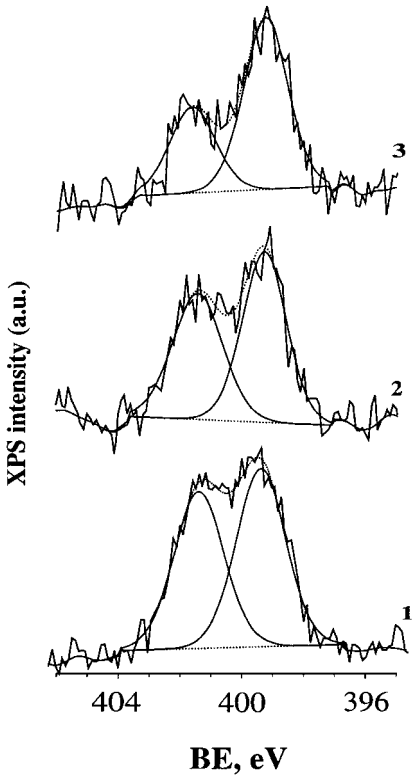

Figure 13. XPS N(1s) spectra of fracture quarz surface conditioned 10 min with HAAc (1) 2×10^{-4} M; (2) 1×10^{-4} M; and (3) the sample (2) after warming at room temperature overnight.

considering the fact that the condition of appearance of the molecular amine at the surface depends on the characteristics not only of the solution but also of the surface (the surface morphology and roughness).

Comparing the DRIFTS (Figures 9 and 10, A and C) and XPS (Table 4) data, one can correlate the disorder−order transfer in the adsorbed layer with the presence of molecular amine and assign this transfer to the point when C_b = CHC.

IRRAS. *Qualitative analysis.* To gain deeper insight into the structure of adsorbed amine, the IRRAS spectra of the quartz surface have been measured at the angles of incidence of 70° and 73°. The 70−73° angle range was found[56,57] to be optimal for orientation characterization employing the ν(CH) bands of an organic molecule present on a silicate surface. As seen from Figures 14 and 15, the s-polarized IRRAS spectra are similar to the DRIFTS spectra. The exceptions are (1) the negative direction of the absorption bands, which is universal for any film on any transparent substrate, because of the so-called "optical effect"[58] and (2) the presence of the bands at 1740−1750, 1650, 1600, and 1547 cm^{-1}. All of these bands (although weak) can be distinguished in the p-polarized spectra. In some cases they disappeared after washing of the sample with water. On the basis of the XPS data, one might assign these bands (or a part of them) to the adsorbed acetate. However, because of these bands are also present in the IRRAS spectra of adsorbed HACl (Figure 15), we assign them tentatively to coadsorbed (bi)carbonate.[59,60] The absence of the corresponding peak in the XPS spectra can be explained by desorption of these species during

(56) Blaudez, D.; Buffeteau, T.; Desbat, B.; Fournier, P.; Ritcey, A.-M.; Pezolet, M. *J. Phys. Chem. B* **1998**, *102*, 99.
(57) Chernyshova, I. V.; Hanumantha Rao, K. Submitted for publication.
(58) Yamamoto, K.; Ishida, H. *Vibrational Spectrosc.* **1994**, *8*, 1.

Table 4. XPS Data on Adsorption of Amines on the Quartz Surface

		element atom % (BE, eV)				
substrate	amine	N	C	O	Si	Cl
fracture surface	2×10^{-4} DAAc	1.23 (400.1)	43.08 (285.0), 3.23 (286.0), 2.12 (288.6)	29.69 (532.8), 2.45 (531.6)	18.2 (103.5)	0
	4×10^{-5} M DACl	1.98 (400.1)	51.12 (285.0), 6.85 (286.5)	26.37 (532.8)	14.48 (103.5)	0
	4×10^{-5} M DACl after heating	1.37 (400.0)	50.27 (285.0), 6.85 (286.5)	25.62 (532.8)	16.02 (103.5)	0
	2×10^{-4} M DACl	2.29 (400.1), 0.55 (401.9)	33.10 (285.0), 3.97 (286.4)	37.31 (532.4), 2.63 (530.7)	20.16 (103.2)	0
	2×10^{-4} M HAAc	0.64 (399.5), 0.54 (401.4)	33.43 (285.0), 3.86 (286.0), 1.57 (288.1)	0.84 (530.8), 37.07 (532.5)	22.02 (103.2)	0
	1×10^{-4} M HAAc	0.39 (399.3), 0.32 (401.5)	23.09 (285.0), 1.95 (286.0)	47.5 (532.5)	26.75 (103.3)	0
	1×10^{-4} M HAAc after heating	0.38 (399.3), 0.20 (401.7)	21.29 (285.0), 2.37 (285.7)	48.74 (532.7)	27.01 (103.4)	0
powder	4×10^{-5} M DAAc	0.39 (400.1)	15.70 (285.0)	54.9	29.01	0
	2×10^{-4} M DAAc	0.35 (399.8), 0.2 (402.0)	16.53 (285.0), 1.48 (286.8), 0.63 (288.6)	53.86	27.24	0
	2×10^{-4} M DACl	0.64 (399.5), 0.24 (401.6)	24.33 (285.0)	49.11	25.66	0.2
	2×10^{-5} HAA	0.38 (399.4), 0.24 (401.6)	19.6 (285.0), 1.56 (286.9), 0.83 (288.6)	51.06	25.88	0

evacuation. The bands at 1650, 1600, and 1547 cm^{-1} can originate from molecular form of amine (Table 3) as well as adsorbed water. The absorption bands of acetate, whose existence at the surface has been demonstrated by the XPS data, are assumed to be overlapped with these "artifact" bands.

The p-polarized spectra of a film on a transparent substrate are more complex due to the fact that each p-polarized spectrum represents the superposition of two spectra: the spectrum of the modes that have the TDM components perpendicular to the surface and the spectrum of the modes whose TDMs are directed along the surface. According to optical theory,[61,62] at the angle of incidence $\varphi = 70°$, which is greater than the Brewster angle ($\varphi_{Br} = 56.1°$), the "perpendicular" bands point downward, while the "parallel" bands upward. Bearing this in mind, examination of the p-polarized spectra shown in Figures 14 and 15 illustrates that apart from the positive ν(CH) bands, the spectra contain the complex broad band in the 2000−4000 cm^{-1} range due to H-bonded ν(OH) and ν(NH) vibrations. The form and the position of this band vary from one spectrum to another, which is explained by the simultaneous different contribution of the positively and negatively going bands, which denies their unambiguous interpretation. Some structure in the 3300-cm^{-1} range can be attributed to the Fermi resonance between the H-bonded bending and stretching vibrations of the N−H and O−H groups. Notice that the intensity of these bands is much higher than that in the corresponding s-polarized spectra, which implies that the TDM of the H-bonded groups are preferentially perpendicular to the surface.

Packing, orientation, and surface coverage were estimated for the layers adsorbed on the plane (polished) surface, whose IRRAS spectra are shown in Figures 14 and 15. A brief description of the procedure described in detail in ref 57 follows. We concluded that the amine tails are highly disordered in the case of C_{16} adsorbed at 2×10^{-5} M and in all the cases of C_{12} amines (Table 5) (below, case 1), based on the $\nu_{as}(CH_2)$ frequencies in the s-polarized spectra, which are higher than 2919 cm^{-1}.[63] At the same time, in virtue of $\nu_{as}(CH_2) < 2919$ cm^{-1}, the C_{16} amines

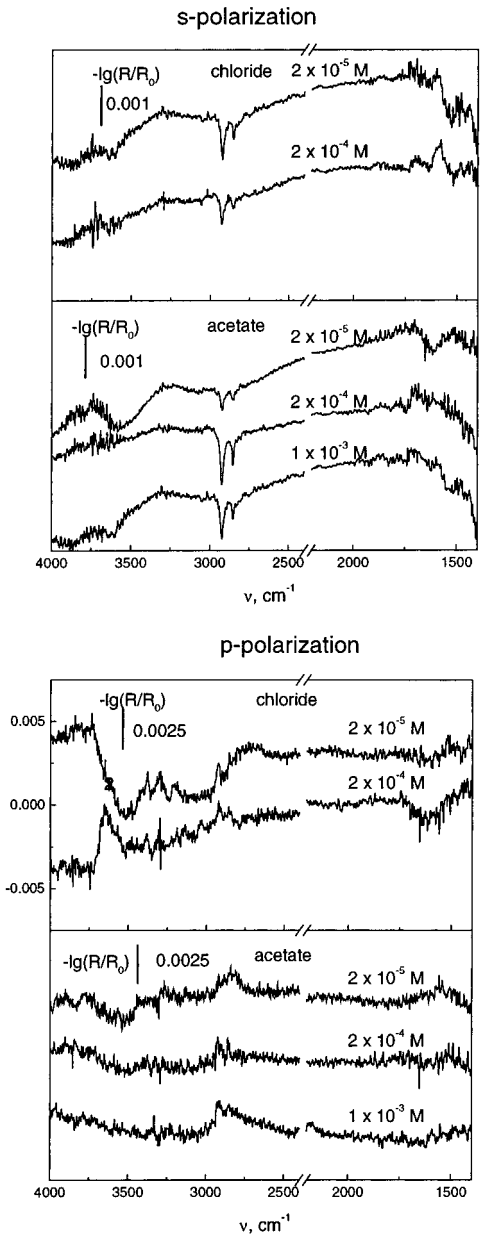

Figure 14. IRRAS spectra of C_{12} amines adsorbed on polished quartz. Amine concentration is indicated on the spectra. The angle of incidence is 70°.

(59) Seiferth, O.; Wolter, K.; Dillmann, B.; Klivenyi, G.; Freund, H.-J.; Scarano, D.; Zecchina, A. *Surf. Sci.* **1999**, *421*, 176.
(60) Parkyns, N. D. *J. Phys. Chem.* **1971**, *75*, 526.
(61) Hoffmann, H.; Mayer, U.; Krischanitz, A. *Langmuir* **1995**, *11*, 1304.
(62) Brunner, H.; Mayer, U.; Hoffmann, H. *Appl. Spectrosc.* **1997**, *51*, 209.
(63) Mendelsohn, R.; Brauner, J. W.; Gericke, A. *Annu. Rev. Phys. Chem.* **1995**, *46*, 305.

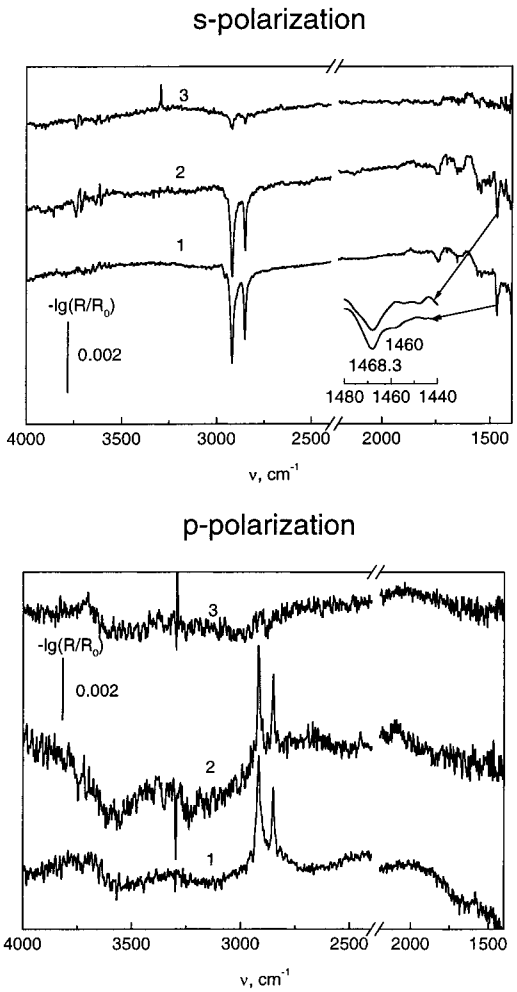

Figure 15. IRRAS spectra of C_{16} amines adsorbed on polished quartz. (1) HACl at 1×10^{-4} M; (2) HACl at 1×10^{-4} M; and (3) HAAc at 2×10^{-5} M. The angle of incidence is (1,2) 73° and (3) 70°. The insert shows details of the $\delta(CH_2)$ band.

adsorbed at the 1×10^{-4} M concentration (below, case 2) are assumed to be in well-ordered phase.[36,64] The ratios of the intensities of the $\nu_{as}(CH_2)$ and $\nu_s(CH_2)$ bands, $A(\nu_{as})/A(\nu_s)$, in the s- and p-polarized spectra (and, what is the same, the dichroic ratios (DR) for the $\nu_{as}(CH_2)$ and $\nu_s(CH_2)$ bands) occurred to be different (Table 5). Therefore, the chain organization in case 2 can be classified[65] as biaxial.

The observed values of DR and $A(\nu_{as})/A(\nu_s)$ (Table 5) were fitted into the corresponding dependences constructed for a biaxial and isotropic monolayer at a quartz surface. The monolayer optical parameters were taken from ref 66 and for quartz from ref 67). The fitting confirms that in case 1 amine tails are practically totally disordered (the theoretical DR for the isotropic organization is 1.1). The exception is DAAc at 1×10^{-3} M, for which $DR_{as} = -0.8$, which, along with the $\nu(CH_2)$ frequencies points to a partial order in the adsorbed layer. In case 2 the observed spectral characteristics fit well into those simulated for the tilt angle of 30°. The biaxiality was found rather low (±10° from the magic[65] (45°) angle. (Note[66] that because of the spectral noise and the uncertainty of the angle of incidence the accuracy in the measured tilt angle is hardly better than 10°.) For comparison, the tilt angle of 30° and the close band positions have been reported for self-assembled monolayers (SAMs) of alkanthiols on gold.[68,69]

A close inspection of the $\nu(CH)$ region in the s- and p-polarized spectra (not shown) does not reveal the $\nu_s^{ip}(CH_3)$ band at 2870 cm^{-1}, which confirms that the tilt angle is close to 30°. As a matter of fact, since the TDM of the $\nu_s^{ip}(CH_3)$ modes is inclined by 35.5° away from the chain axis (Figure 2) at the chain tilt angle of 35.5° it is perpendicular to the substrate surface. Under this condition, the corresponding absorption band will be absent in the s-polarized spectrum and negative in the p-polarized spectrum (the latter feature was not distinguished due to the low SNR). With the known orientation, the surface coverage can be calculated. The results are collected in Table 5.

In case 2 we observe that the $\delta(CH_2)$ band splits into two components: 1468.3 and 1460 cm^{-1} for HAAc and 1468 and 1474 (shoulder) cm^{-1} for HACl (insert in Figure 15). Keeping the above results in mind and the rhombic positioning of oxygen atoms at the (002) quartz plane, we suggest that the molecules adopt monoclinic-like packing; however, the presence of tilted hexagonal phase responsible for the 1468-cm^{-1} component cannot be totally excluded.

Thus, the main conclusion from the IRRAS data is that at $C_b <$ CHC (case I) the adsorbed species are almost totally disordered, while at $C_b >$ CHC (case II) they become highly ordered in a monoclinic subcell, in which the hydrogen−carbon chains (of C_{16} amines) are inclined by 30° from the surface normal. The orientation of the H-bonded amine headgroups and/or silanol groups is such that their TDMs are preferentially perpendicular to the surface.

The spectroscopic results obtained allow us to divide adsorption of amine on quartz into three qualitatively different regions (in the brackets the source of the conclusion is indicated): (1) at $C_b <$ CHC (region I) surface silanol groups interact with ammonium groups through H-bonds eq 2 (DRIFTS, IRRAS, and XPS), the hydrocarbon chains of adsorbed amine have chaotical orientation (IRRAS, DRIFTS); (2) at CHC $\leq C_b < C_{pr}$ (region II), the content of the adsorbed layer changes—instead of species described by eq 2, molecular amine and protonated amine coordinated to anion (eq 1) dominate at the quartz surface (XPS), covering it only partially (the E curves in Figures 9 and 16) and the hydrocarbon chains become highly organized (IRRAS and DRIFS); (3) at $C_b \geq C_{pr}$ (region III), bulk amine precipitates (DRIFTS); (4) processes in regions II and III are effected by the amine counterion (XPS).

ζ Potential and Flotation. The ζ potential curves follow the corresponding A_n curves (Figures 9 and 10, A). In regions II and III ζ potential of quartz reacted with the amine acetate solutions is lower than that in the case of the chlorine salts (Figures 9 and 10, C). This fact should be regarded as a consequence of lesser adsorption of amine in the presence of acetate ions. Since in these regions neutral molecules are adsorbed in the first monolayer and then as bulk precipitates, the effect of coadsorption of acetate ions does not reduce to rendering the surface charge more negative: the presence of acetate ions in the double layer suppresses the formation of neutral molecules (precipitation). Another conclusion is that increasing ζ potential here is not due to adsorption of cations, as has

(64) Gericke, A.; Huhnerfuss, H. *J. Chem. Phys.* **1993**, *97*, 12899.
(65) Ahn, D. J.; Franses, E. I. *J. Phys. Chem.* **1992**, *96*, 9952.
(66) Buffeteau, T.; Blaudez, D.; Pere, E.; Desbat, B. *J. Phys. Chem. B* **1999**, *103*, 5020.
(67) Palik, E. D. *Handbook of Optical Constants of Solids*; Academic Press: New York, 1998.
(68) Sinniah, K.; Cheng, J.; Terrettas, S.; Reuttrobey, J. E.; Miller, C. J. *J. Phys. Chem.* **1995**, *99*, 14500.
(69) Hoffman, H.; Mayer, U.; Brunner, H.; Krischanitz, A. *Vibrational Spectrosc.* **1995**, *8*, 151.

Table 5. Characteristics of the Adsorded Layers, Taken from the IRRAS Spectra Shown in Figures 14 and 15

amine, conc	$\nu_{as}(CH_2)$, cm^{-1} [a]	$\nu_s(CH_2)$, cm^{-1}	DR_{as} [b]	DR_s [c]	$\left(\frac{A(\nu_{as})}{A(\nu_s)}\right)^s$	$\left(\frac{A(\nu_{as})}{A(\nu_s)}\right)^p$	no. of monolayers
DACl, 2×10^{-5} M	2921.8	2850.9	−1 [d]	*d*	1.8		0.69
DACl, 2×10^{-4} M	2924.7	2853.8	−1	*d*	1.9		0.42
DAAc, 2×10^{-5} M	2922.6	2855.4	−1	*d*	1.7		0.35
DAAc, 2×10^{-4} M	2922.7	2853.4	−1	*d*	2.0		0.82
DAAc, 1×10^{-3} M	2921.9	2852.0	−0.8	*d*	2.0		0.65
HACl, 2×10^{-5} M	2921.7	2851.7	−0.8	*d*	1.3?		0.27
HACl, 1×10^{-4} M	2918.4	2850.8	−0.69	−0.62	1.56	1.40	1.0
HAAc, 1×10^{-4} M	2918.3	2850.9	−0.62	−0.72	1.38	1.62	1.0

[a] The band maximum in the s-polarized spectra. [b] Dichroic ratio for the $\nu_{as}(CH_2)$ band. [c] Dichroic ratio for the $\nu_s(CH_2)$ band. [d] The value is questionable due to low SNR.

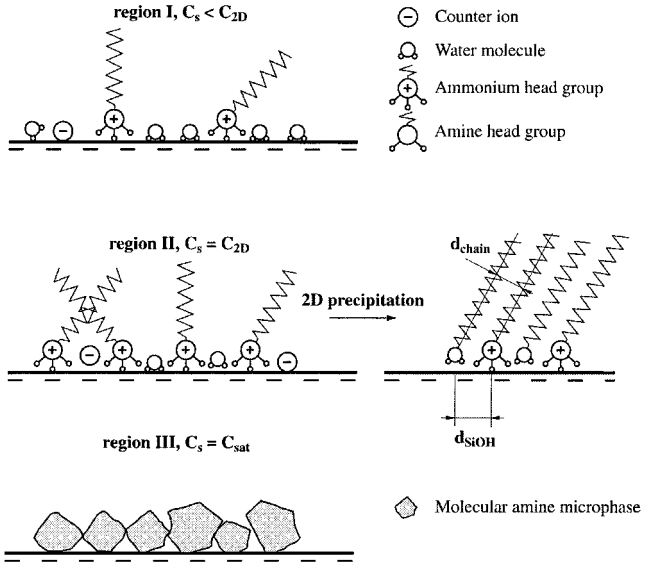

Figure 16. Adsorption according to the 2D−3D precipitation mechanism.

been suggested by examining only the ζ potential curves and adsorption isotherms in the absence of spectroscopic data,[6−8] but is really due to precipitation of molecular amine. The fact that the ζ potential of amine colloidal precipitates is positive and increases with increasing amine solution concentration has been reported by Laskowski et al.[70]

In contrast, the flotation results appear to be independent of the origin of the amine counterion. We attribute this effect to surface *inhomogeneity*: for flotation of the particle to happen, it is sufficient that its surface has one highly hydrophobic patch.

Discussion

Before discussing the results the HM and CT are examined in more detail below.

The HM is based on the following facts. The relationship between the bulk concentration C_b and concentration of cations at the "negatively charged mineral/water" interface, C_s, is given by the Boltzmann equation:[6]

$$C_s = C_b \exp(-F\psi_i/RT) \qquad (3)$$

Here, ψ_i is the potential in the plane where the physically adsorbed ions are positioned. Taking $\psi_i = -135$ mV as average of the measured ζ potential of the initial quartz (−80 mV) and the approximated value of the double layer potential of quartz at pH 7 (−190 mV),[6] it was shown[6] that for $C_b = 1 \times 10^{-4}$ M, around which the break in the adsorption characteristics is observed, amine concentration at the interface ($C_s = 0.02$ M) is close to CMC of dodecylammonium chloride (DACl) (0.014 at 30 °C).[4]

Furthermore, the free energy of transfer of one CH_2 group from solution to a hemimicelle was estimated as follows.[12,71] According to Grahame's version of the Stern isotherm, the adsorption density of the surfactant Γ_+ (ions cm^{-2}) is described by

$$\Gamma_+ = 2rC_b \exp(-\Delta G_{ads}{}^0/kT) \qquad (4)$$

where *r* is the radius of the adsorbed ion. The total adsorption energy $\Delta G_{ads}{}^0$ can be divided into electrostatic term $ze\psi_i$ (*z* is the ion valency and *e* is electron charge); a term for interaction of the headgroup with the surface, ϑ_{HG}; and the van der Waals cohesive (adsorption) free energy between hydrocarbon chains, $n\Delta\omega$ (*n* is the number of the CH_2 groups in the chain, $\Delta\omega$ is the attractive (lateral) energy per one CH_2 group):

$$\Delta G_{ads}{}^0 = ze\psi_i + \vartheta_{HG} + n\Delta\omega \qquad (5)$$

Differentiation with respect to ln C_b and rearrangement of eq 4 yields for the point of the charge reversal, C_{pcr}, when $\psi_i = 0$:

$$\ln C_b = \left(\ln \Gamma_+ - \ln 2r + \frac{\vartheta_{HG}}{kT}\right) + n\frac{\Delta\omega}{kT} \qquad (6)$$

Assuming the term in parentheses constant at the pcr (i.e., *independent* of the surfactant chain length), the value of $\Delta\omega$ is obtained from the slope of the dependence of ln C_{pcr} on *n*. For a homologue series of $C_{10} - C_{18}$ alkylamine acetates, $\Delta\omega = 0.97kT$. This value agrees excellently with the cohesive energy per one CH_2 group in bulk micelles ($1 - 1.1kT$). This fact has been regarded as a confirmation of validity of the HM basic hypothesis.[7,10]

However, this coincidence can be doubted because of the following reasoning. One can calculate using eq 3 the surface concentration of amine C_s^{pcr} for $C_b = C_{pcr}$, taking the reported[7] points of charge reversal of quartz in solutions of amines with different chain lengths and initial (in pure water) ζ potential $\zeta = -60$ mV. The results are shown in Table 6. On the other hand, at given pH = 6.5 and $pK_a = 10.6$ (this value is approximately the same for all the long-chain amines[4]), the saturation concentration C_{sat} is given by[13]

$$\log C_{sat} = \log C_{sol} + 4.13 \qquad (7)$$

where C_{sol} is solubility limit. For values of C_{sol} taken from Smith,[3] the calculated values of C_{sat} are also listed in Table

(70) Laskowski, J. S.; Vurdela, R. M.; Liu, Q. *Proceedings of the 16th International Mineral Processing Congress*; Eric Forssberg, K. S., Ed.; Elsevier: Amsterdam, 1988; pp 703−715.

(71) Fuerstenau, D. W.; Healy, Th. W.; Somasundaran, P. *Trans. Soc. Mineral Eng. AIME* **1964**, *229*, 321.

Table 6. Critical Concentrations for DA Aqueous Solutions at pH 6.5

no. of C atoms in alkyl chain	log C_{sol}[3]	log C_{sat}	log C_{pcr}[7]	log C_s^{pcr}
10	−3.3	0.83	−1.40	0.69
12	−4.7	−0.57	−1.89	0.2
14	−6.0	−1.87	−2.49	−0.4

6. One can see that for amines with the chains more than 10 carbon lengths $C_s^{pcr} > C_{sat}$. It follows that at C^{pcr} these amines exist at the quartz surface as precipitated phase implying that the above-mentioned procedure of estimation of $\Delta\omega$ is incorrect and the coincidence of $\Delta\omega$ for this case should have another physical meaning.

One can see that the results obtained are inconsistent in all the adsorption regions with the HM model,[6,9] which ignores a possibility of specific bonding between the surfactant headgroup and the adsorption site and the possibility of any precipitation. Table 3 gives an additional confirmation of this statement: the surface coverage at $C_b = C_{pcr}$ depends not only on the chain length but also on the origin of the counterion, which contradicts with the basic assumption made by Somasundaran et al.[7,12,71] Since the coverage of the well-organized layer of HA, which is formed at $C_b = 1 \times 10^{-4}$ M, is about one monolayer (Table 5), the AT seems also inapplicable to the case under examination.

As distinct to the HM, the CT takes into account the possibility of the 2D−3D condensation, describing the adsorption of a surfactant onto an ideal homogeneous surface by the so-called Cases−Mutaftschiev isotherm:

$$kT \ln\left(\frac{C_b}{C_{ref}}\right) = (\vartheta_0 - \vartheta_a) - \frac{\omega}{2}(1 - 2\theta) + kT \ln \frac{\theta}{1 - \theta} \quad (8)$$

Here, $\theta = [SA]/[S_T]$ is the surface coverage (SA is the concentration of the adsorbate on surface sites, $[S_T]$ is the maximum concentration of surface sites); $C_b$is the equilibrium bulk concentration for a given θ; C_{ref} is the saturation concentration for the *reference phase* (see below); ϑ_a is the potential of interaction between the headgroup and the adsorption site (this can be specific ϑ_{HG} (chemical or H-bonding) or electrostatical $ze\psi_i$ (see eq 5); ϑ_0 is the potential of binding of the surfactant headgroup in the reference phase; and ω is the sum per molecule of lateral interactions in the adsorbed layer at $\theta = 1$. The reference phase is "the hydrated crystal" or micelles in equilibrium with monomers for $T < T_K$ or $T > T_K$, respectively. Under the term "hydrated crystal", the CT implies "a lamenar structure, with the polar groups lying along the interface with water. The arrangement is such that the hydrocarbon chains are perpendicular to the interface and each sheet is approximately two hydrocarbon chain lengths thick... The space between sheets is mainly occupied by water and counterions".[20]

The parameter ω in eq 8 can be approximated as

$$\omega = n\Delta\omega - \omega_{rep} \quad (9)$$

where the term $n\Delta\omega$ has the same meaning as in eq 5 and ω_{rep} is the energy of repulsion between the polar groups. For a surfactant with more than nine carbon atoms in the alkyl chain, lateral interactions ω are higher than the critical value of lateral bonds $4kT$. In this case eq 8 transforms into the well-known Frumkin equation for the isotherm of 2D condensation of an adsorbent onto a homogeneous surface, which is depicted in Figure 1, A. The abrupt jump in the isotherm corresponds to the condition

$$kT \ln \frac{C_b^*}{C_{ref}} = \vartheta_0 - \vartheta_a \quad (10)$$

where C_b^* is the critical bulk concentration, which can be expressed as:

$$kT \ln C_b^* = -n\Delta\omega/2 - \vartheta_a + \omega_{rep}/2 + \text{constant} \quad (11)$$

It is seen that increasing hydrophobic interaction (the first term in the right side of eq 11) and increasing bonding with the adsorbent (the second term) results in decreasing the critical concentration. At $C_b < C_b^*$ the adsorbent is predicted to be sparsely populated by chaotically oriented monomers, while at $C_b > C_b^*$ the 2D condensed monolayer forms.

In our opinion, most of the experimental data obtained can be interpreted within the framework of the CT if one assumes that at CHC instead of the 2D condensation *2D precipitation* of amine takes place. The difference between 2D precipitation and 2D condensation consists of that in the first case the reference phase is represented by molecular crystal, while in the second case by the hydrated crystal. Both the models become formally the same if one assumes that $C_{ref} = C_{sat}$ in eqs (8) and (10). In the 2D-precipitated monolayer the headgroups are H-bonded with surface silanols, and equilibrium (2) is established. It means that the ionic-molecular species suggested by Laskowski[13] for solution do exist at least in the 2D space at the interface. Since at the surface the ionic headgroups are surrounded by the deprotonated ones, the electrostatic repulsion between them decreases due to screening, and as a result, dense packing and ordered orientation of adsorbed amine becomes possible. This effect seems not to be restricted to the case of long-chain primary amines. A higher thermodynamical stability of molecular as compared to ionic species has been reported[72] for fatty acids in form of a Langmuir monolayer at the water/air interface: $pK_a \approx 11$ for the arachidic acid monolayer, while $pK_a \approx 6$ in an aqueous solution.

As saturation concentration C_{sat} is reached at the mineral−solution interface, the bulk (3D) precipitation of the amine begins.

A mechanism of the successive 2D and 3D precipitation (2D−3DP) of alkylamines on quartz surface is proposed and is illustrated by Figure 16. If this mechanism is qualitatively adequate the following two conditions have to be satisfied: (1) there should be geometric possibility for formation of the densely packed layer of alkylamine on the quartz surface and (2) the surface concentration of amine at CHC has to be critical concentration at which 2D saturation is possible.

As a matter of fact, each hydroxyl on the quartz surface occupies ca. 0.234 nm^2,[2,73] while the cross-sectional area of each hydrocarbon chain in a close-packed monolayer (all-trans hydrocarbon chains), d_{chain}, which one should expect to form at CHC, is ca. 0.19−0.20 nm^2.[64,74] Formally, with packing one amine per 0.234 nm^2 and $\gamma = 30°$, one can obtain that the actual cross-sectional area of the HA species is 0.20 nm^2 (Figure 16, region II), which excellently agrees with the values of d_{chain} for densely packed SAMs and the Langmuir monolayers in solid phase. This rough estimation demonstrates that there is geometric possibility

(72) Oishi, Y.; Takashima, Y.; Suehiro, K.; Kajiyama T. *Langmuir* **1997**, *13*, 2527.

(73) Iler, K. R. *The Chemistry of Silica: Solubility, Polymerization, Colloid and Surface Properties, and Biochemistry*; John Wiley and Sons: New York, 1979.

(74) Dluhy, R. A. *J. Phys. Chem.* **1986**, 90, 1373.

for the formation of a densely packed layer of alkylamine on the quartz surface.

Since at the moment the microscopic theoretical calculations are not available, it is not clear which concentration should be regarded as the 2D saturation limit. As zeroth approximation, one can evaluate this quantity using the macroscopic (may be ideologically incorrect) interpretation of this term as

$$C_{2D} = C_{sat} N_A d_m, \quad (12)$$

where C_{sat} is the 3D saturation limit, N_A is Avogadro's constant, and d_m is the monolayer thickness. Taking C_{sat} = 0.27 M from Table 6 for DA and assuming that d_m is equal to the DA molecule length (1.62 nm[57]) one can obtain $C_{2D} = 2.6 \times 10^{13}$ molecule/cm^2, which agrees satisfactorily with (is the average of) the values of 4.2×10^{13} [8] and 6×10^{12} [75] molecules/cm^2 given in the literature for the adsorbed density of DAAc at CHC.

The foregoing speculations have been made for a homogeneous surface, when the potential gradient is perpendicular to the surface. However, all real-world surfaces are rough and inhomogeneous, especially those of the ground particles. Thus, one can expect the gradient to be distributed along the surface, being greater at the surface patch, where the surface concentration of the adsorption sites is higher. As a result, the 2D precipitation occurs in the regime that is qualitatively the same as 2D condensation, yielding the substeps on the adsorption isotherm (Figure 1, B), which we have not resolved because of the large steps in changing C_b. However, we regard as testimony to the patch-by-patch adsorption the facts that CHC is higher for the fracture (relatively homogeneous) surface as compared to CHC for the surface of the finely ground particles and the indifference of the flotation results from the origin of the amine counterion.

We see the following deficiencies in the interpretation of the results obtained. At the ζ potential of the initial quartz powder (−33 mV), eq 4 gives that solubility limit of DA (Table 6) is reached at the interface at $C_b = C_{sat}^s \approx 3.7 \times 10^{-3}$ M, which is 1.8-fold higher than the experimental value of C_{pr} for DACl, while for DAAc C_{pr} is not reached at all (Table 3). As a tentative explanation, one could connect this phenomenon with the surfactant pre-aggregation with the counterion in solution when C_b approaches C_{sat}. Moreover, it is not clear why the quantity of DACl adsorbed at the polished surface from the 4×10^{-5} M solution is higher than that from the 2×10^{-4} M solution (Table 5 and Figure 14) (this result was reproduced).

General qualitative comments may be as follows. The complexity of the "amine−surface" interaction is such that one-to-one transfer of the CT to the case of successive precipitation of amine is incorrect: at $C_b >$ CHC in the first monolayer, molecular as well-protonated amine is present, while the surfactant counterion somehow affects amine aggregation. This problem requires a separate further theoretical and experimental study.

Notice that if the surfactant (amine) monolayer is formed according to the 2DP mechanism, rapid *self-assembly* takes place (for the C_{16} amine for the time shorter than 5 min). For comparison, adsorbed $C_{18}TA^+$ ions on mica are aggregated by the pure "hydrophobic effect" (when the 2DP mechanism does not work) into the 2D solid patches only after 168 h exposure to the $C_{18}TA^+$ solution.[33]

Finally, note that the analogous study of amine adsorption on albite[76] showed that this mechanism seems to be universal in regard to the amine−silicate system.

Conclusions

The mechanism of adsorption of long-chained amines at pH 6−7 onto quartz has been studied using the direct methods, FTIR and XPS spectroscopy, and correlating the spectroscopic data with the data of the indirect methods- ζ potential measurements and flotation tests. As a result, the adsorption characteristics were split into three regions. At amine concentration $C_b <$ CHC (region I) surface silanol groups interact with the ammonium headgroups through H-bonds (eq 2), while the hydrocarbon chains have chaotical orientation. At CHC $\leq C_b < C_{pr}$ (region II) the content of the adsorbed layer qualitatively changes: instead of species eq 2, molecular amine H-bonded to surface silanol and protonated amine coordinated to deprotonated silanol oxygen (eq 1) appear at the quartz surface, due to this fact adsorption steeply increases and the hydrocarbon chains become highly organized (in the monolayer of HA adsorbed at the polished surface the tilt angle is about 30°). At $C_b \geq C_{pr}$ (region III) bulk amine precipitation takes place. Formation of neutral molecules in both regions II and III is affected by the amine counterion.

It has been demonstrated that these data are inconsistent with the hemimicelle model and admicelle theory, while can be qualitatively partially interpreted within the framework of the condensation theory of Cases et al.[20] if one substitute the phenomenon "condensation", which this theory deals with, by the phenomenon "precipitation".

Acknowledgment. I.V.C. gratefully acknowledges the financial support of The Swedish Institute, Stockholm.

LA000254Y

(75) de Bruyn, P. L. *Trans Soc. Mineral Eng. AIME* **1955**, *202*, 291.
(76) Chernyshova, I. V.; Hanumantha Rao, K.; et al. Submitted for publication.
(77) Ihs; A.; Liedberg, B.; Uvdal, K.; Tornkvist, C.; Bodo, P.; Lundstrom, I. *J. Colloid Interface Sci.* **1990**, *140*, 192.
(78) Bellamy, L. J. *The Infared Spectra of Complex Molecules*; Wiley: New York, 1975.
(79) Przeslawska, M.; Melikowa, S. M.; Lipkowski, P. *Vibrational Spectrosc.* **1999**, *20*, 69.